Solid State Science and Technology, Vol. 22, No 1 & 2 (2014) 101-110
ISSN 0128-7389 | *http://journal.masshp.net*

MAGNETIC AND TRANSPORT PROPERTIES OF $LaMnO_3$/$La_{0.67}Ba_{0.33}MnO_3$ SINGLE AND BI-LAYER THIN FILMS

K. P. Lim[1], J. K. Wong[1], S. A. Halim[1], S. K. Chen[1], S. W. Ng[1] and H. S. Woon[2]

[1]*Department of Physics, Faculty of Science, Universiti Putra Malaysia, 43400 UPM Serdang, Selangor, Malaysia.*

[2]*College of Engineering, Universiti Tenaga Nasional, Jalan IKRAM-UNITEN, 43000 Kajang, Selangor, Malaysia.*

Corresponding author: kplim@science.upm.edu.my

ABSTRACT

Single and bi-layer thin films of $LaMnO_3$ and $La_{0.67}Ba_{0.33}MnO_3$ were deposited on amorphous fused silica substrate via pulsed laser deposition technique (PLD). In this work, the effect of stacking sequence in bi-layer manganite films of $LaMnO_3$ and $La_{0.67}Ba_{0.33}MnO_3$ was reported. The crystal structure formation, magnetic, resistivity and magnetotransport properties of bi-layer manganite films were studied. The unit cell of LMO undergo negative misfit when growth on LBMO while positive misfit for unit cell of LBMO when growth on LMO. Such changes indirectly alter the magnetism of the system since it governed by the Mn-O-Mn bond angle and Mn-O bond length. Therefore, different magnetic pinning strength was observed between the LMO and LBMO layer coupled in LMO/LBMO and LBMO/LMO respectively. The stronger the magnetic spins pinning effect, the higher the resistivity is and the more scattered the %MR are.

Keywords: colossal magnetoresistance; thin film; manganite; crystal structure; magnetism

INTRODUCTION

The discovery of Colossal Magnetoresistance (CMR) had stimulated many interests not only for the fundamental sciences but also potential application in magnetic sensor industries [1]. Conventionally, most of these materials are often prepared in thin films system [2]. Therefore, many work had been done on single magnetic layer [3-6] and fewer studies are on bi-layer or superlattices manganite oxide films. The magnetoresistance arises from spin dependent transmission of the conduction electrons via those layers with enhanced magnetoresistance [7]. However, the properties of manganite thin films are different especially its magnetic or magnetotransport properties. Therefore, investigation of structure, magnetic and magnetotransport of single and bi-layer thin film of $LaMnO_3$ and $La_{0.67}Ba_{0.33}MnO_3$ manganite were reported.

Solid State Science and Technology, Vol. 22, No 1 & 2 (2014) 101-110
ISSN 0128-7389 | *http://journal.masshp.net*

METHOD

Conventional solid state reaction technique was used to prepare bulk $LaMnO_3$ and $La_{0.67}Ba_{0.33}MnO_3$ pellet. Stoichiometric amount of La_2O_3, $BaCO_3$ and $MnCO_3$ starting powder were mixed and wet milled in acetone. The milled powders were dried and ground before calcine at 900°C for 12 hours. The powders were reground, sieved and pressed into pellet before sinter at 1300°C for 24 hours. To fabricate thin film, Pulsed Laser Deposition (PLD) technique was used to convert the fabricated bulk pellet into thin film on amorphous fused silica substrate (JGS1). The Nd-YAG laser with wavelength of 1064nm and energy of 1.5 J/pulse at a pulse repetition rate of 10 pps was utilized. Initially, the substrate which located 4 cm parallel to the target was stabilized at 400°C in the oxygen pressured of 7×10^{-2} mbar. The deposition was carried out by focused laser beam on the rotating target in power density about 4.7×10^{5} W/cm^2 and the deposition interval was half an hour. The film was cooled down slowly and trapped in surrounding of 2 mbar oxygen before post anneal in air at 700°C for 4 hours. Under this condition, single layer thin films of $LaMnO_3$ (LMO) and $La_{0.67}Ba_{0.33}MnO_3$ (LBMO) and bi-layer thin films from the coupling of LMO and LBMO were fabricated. The bi-layer films are LMO growth on LBMO layer to form LMO/LBMO and vice versa for LBMO/LMO.

X-ray diffraction (XRD, Phillips PW 3040/60 Xpert Pro) technique was used to analysis the phase and crystal structure embedded in films. The collected data were analyzed using Rietveld refinement technique with X'Pert HighsScore Plus program. The microstructures were analyzed using Field Emission Scanning Electron Microscope (FE-SEM, Zeiss SUPRA^{TM} 55VP and JEOL JSM-6701F). The magnetic properties were measured with Vibrating Sample Magnetometer (VSM, Lakeshore 7400 series) while the electrical transports were examined by Hall Measurement System (Lake Shore 7604 Hall Measurement System) in a cryostat with temperature range from 80 K to 300 K in 0T to 1T magnetic field, respectively.

RESULTS AND DISCUSSIONS

Figure 1 shows the detectable XRD spectra of all single phase thin film samples. The XRD data of all samples were refined with Rietveld refinement technique. The refined crystallography data were computed and tabulated in Table 1. Orthorhombic crystal structure with space group of *Pnma* was observed from all samples. Negative misfit was observed from the unit cell of LMO in LMO/LBMO while positive misfit on LBMO in LBMO/LMO. Indeed, smaller unit cells (*a* and *b* axis) of LMO were growth on bigger unit cell of LBMO and vice versa for LBMO growth on LMO. Lattice misfit take place and generated lattice strain which could alter the system especially the crystal structure of top layer. Such effect indirectly alters the Mn-O-Mn bond angle and Mn-O bond length of Mn-O-Mn chains while revolutionize to lattice parameter, volume and density of the unit cell (Table 1). Moreover, smaller crystallite size was observed from greater strained system. These show the influence of stacking sequence in crystal structure

growth as the characteristic of top layer is interrelated to the bottom layer of bi-layer thin film to be growth. Schematic draw as shown in Figure 2 illustrate the changes in crystal structure of all samples.

Table 1: Refined crystallography data of LMO, LBMO, LBMO/LMO and LMO/LBMO thin films

Sample	**LMO**	**LBMO**	**LBMO/LMO**	**LMO/LBMO**
Crystal System	---------- Orthorhombic ----------			
Space Group	---------- *Pnma* ----------			
Lattice parameter				
***a* (Å)**	5.452 (2)	5.516 (2)	5.513 (2)	5.458 (3)
***b* (Å)**	7.725 (3)	7.786 (2)	7.781 (3)	7.729 (5)
***c* (Å)**	5.521 (2)	5.562 (4)	5.569 (1)	5.525 (2)
Volume ($Å^3$)	232.526	238.874	238.891	232.497
Density (g/cm^3)	6.908	6.740	6.714	6.815
Crys. Size, D (nm)	21.8	14.0	16.6	11.9
Lattice strain (%)	0.628	0.954	0.815	1.100
Mn-O(1)-Mn (°)	161.0 (3)	162.9 (3)	151.3 (8)	158.0 (7)
Mn-O(2)-Mn (°)	166.4 (4)	159.9 (5)	148.5 (3)	162.3 (9)
Mn-O(1) (Å)	1.812 ×2 2.121 ×2	1.892 ×2 2.069 ×2	1.830×2 2.203×2	1.892×2 2.061×2
Mn-O(2) (Å)	1.945 ×2	1.977 ×2	2.021×2	1.954×2
Goodness of fit	1.541	1.217	1.329	1.522

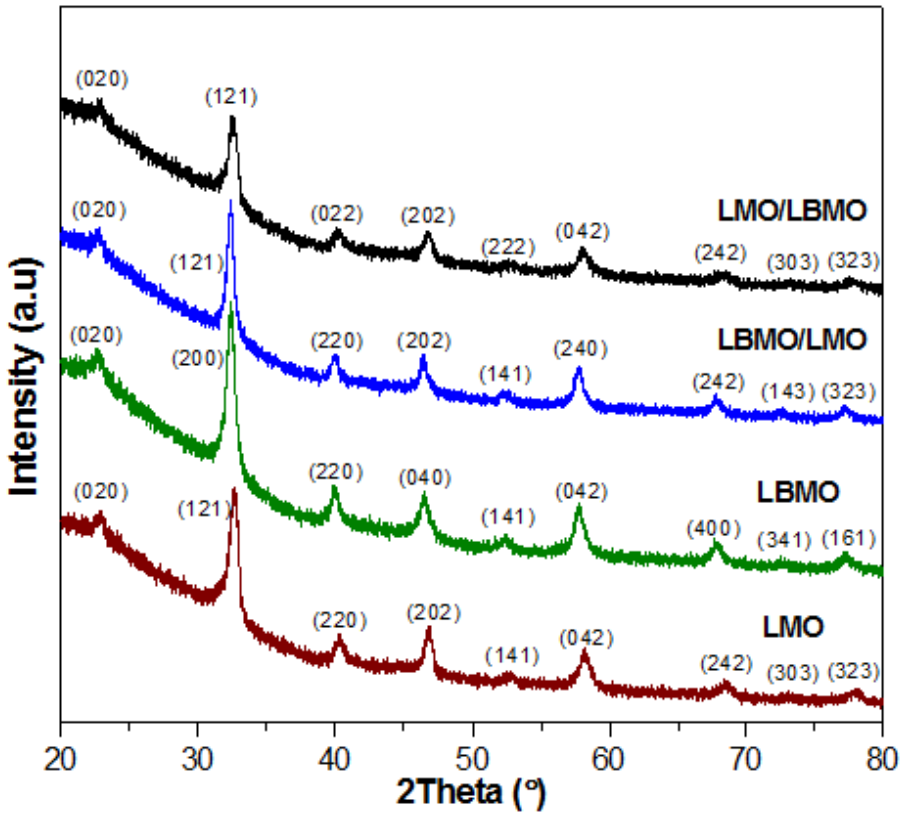

Figure 1: XRD spectra of LMO, LBMO, LBMO/LMO and LMO/LBMO thin films

SEM micrographs of all thin film samples as shown in Figure 3 shows the agglomeration of small particles (<100nm) and necked due to strong diffusion to form grain. Layer and Island growth mode was observed. Indeed, the microstructure formation is initially layer-by-layer growth and due to lattice misfit between film and substrate, strains were created and lead to island like growth (rounded pile of grains). Overall, no significant change in microstructure can be seen.

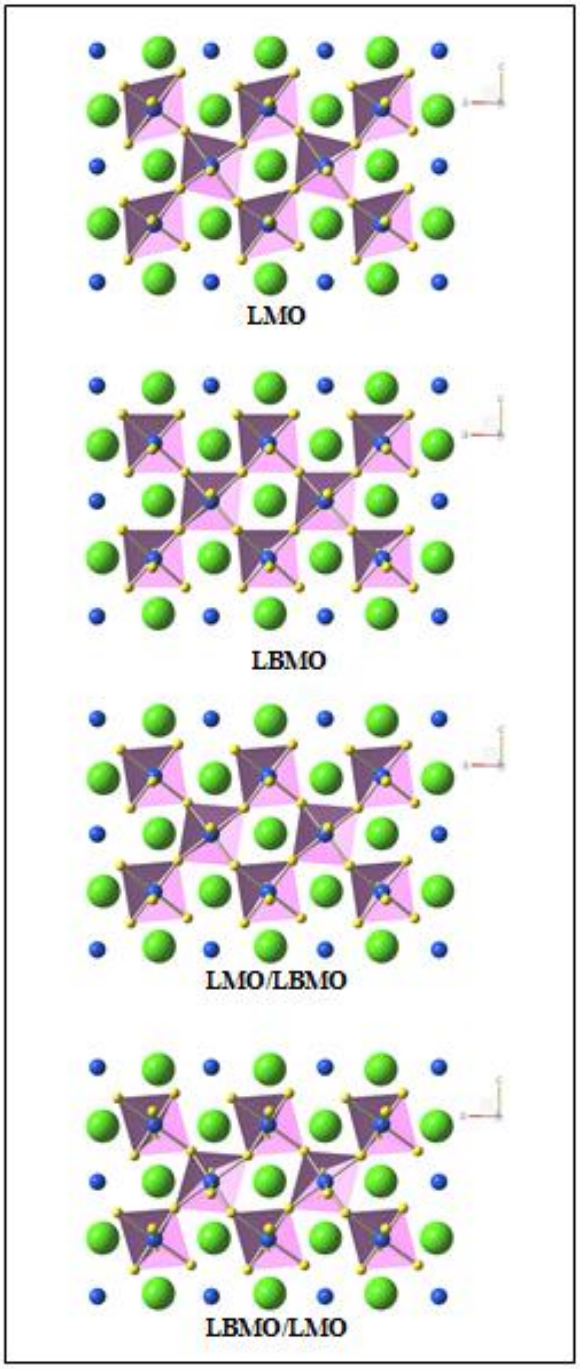

Figure 2: Schematic draw of crystal structure in LMO

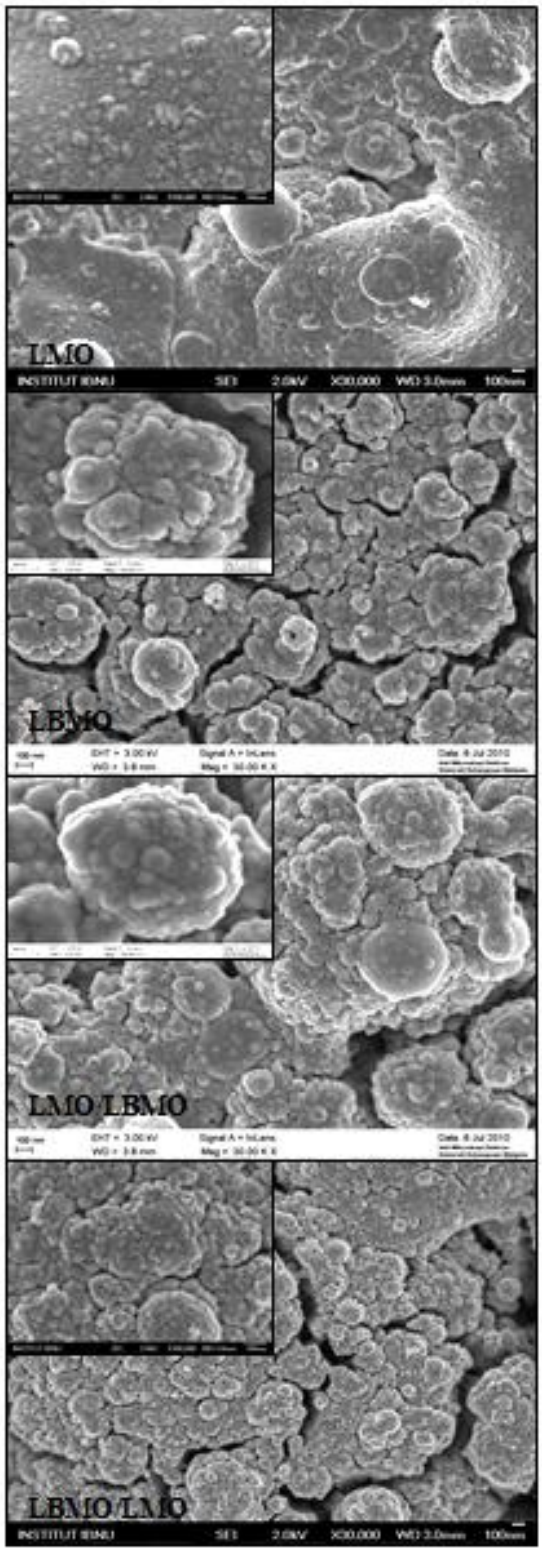

Figure 3: FE-SEM micrographs of LMO, LBMO, LBMO, LMO/LBMO and LBMO/LMO thin films. LMO/LBMO and LBMO/LMO thin films with magnification of 30,000X, the inset was 100,000X

The hysteresis loops as shown in Figure 4 of all sample shows ferromagnetic behavior (sigmoid shape) except LMO which is paramagnetic at room temperature. In applied external magnetic field up to 10kG, the highest resultant magnetization is given by LBMO, LBMO/LMO, LMO/LBMO and LMO with 3.09, 2.42, 1.75 and 0.45 emu/g respectively. The resultant magnetization of bi-layer films are relatively smaller as compared to LBMO, the ferromagnetism shown by LBMO was weakened when coupled with LMO. This might due to the magnetic spins in system suffer from pinning effect in LMO and LBMO coupling [8]. The magnetic spins struggle and unable fully align under applied external magnetic field. Moreover, the resultant magnetization of LBMO/LMO is larger than LMO/LBMO and unlike from each other. In fact, their structure can be viewed as magnetically ordered small regions implanted in a matrix of disordered spins so-called 'cluster' glass state. The change in crystal structure (Mn-O-Mn bond angle and Mn-O bond length) could alter the magnetism of the system [10]. As LBMO growth on LMO layer to form LBMO/LMO, there is a tendency for LBMO to mimic LMO crystal structure due to lattice misfit (see Figure 2). Hence, LBMO become more paramagnetism rather than ferromagnetism due to its disordered state. Similarly, the paramagnetic LMO become more ferromagnetic (weak ferromagnetic) when growth on LBMO layer in LMO/LBMO. The weak ferromagnetism from LMO layer and strong ferromagnetism from LBMO layer could either enhance the resultant magnetization or destroy each other. However, the resultant magnetization value obtained from LMO/LBMO is lower compared to single layer LBMO or LBMO/LMO. Therefore, the magnetic pinning effect was great in LMO/LBMO compared to LBMO/LMO.

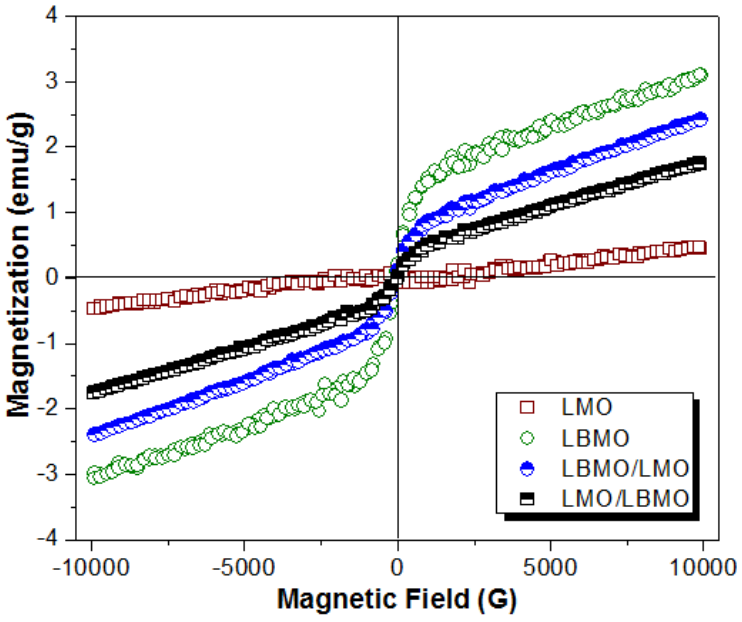

Figure 4: Hysteresis loops of LMO, LBMO, LBMO/LMO and LMO/LBMO thin films taken at room temperature

The temperature variation of resistivity as shown in Figure 5(a) was measured in zero magnetic field. All samples are insulator like with no transition temperature, T_P can be seen and hence might locate below 80K. The highest resistivity was observed from LMO/LBMO followed by LBMO/LMO and LBMO. The resistivity for LMO was not shown since it was an antiferromagentic insulator with very high resistance [F]. In manganite materials, the conduction mechanism was governed by double exchange (DE) mechanism and Jahn-Teller distortion. Via DE, the electron was transfer between Mn^{3+} ($t_{2g}^3 e_g^1$) and Mn^{4+} ($t_{2g}^3 e_g^0$) intrinsically and extrinsically, respectively. Therefore, the mobility of the delocalized spin (e_g) is one of the key for conduction. Upon interrupted, the conduction will disturbed and give rise in resistivity. Such observations best to describe the high resistivity of LMO/LBMO as shown in Figure 5(a). As discussed previously, the strong magnetic pinning effect in LMO/LBMO could decrease the mobility of the spins in the system as well as immobilized it. Thus, limit the electron conduction and give rise in high resistivity. However, this effect was weak in LBMO/LMO since the magnetic pinning effect is weaker (higher magnetization) and hence the resistivity is slightly lower as compared to LMO/LBMO while LBMO have the lowest resistivity since it no suffer any magnetic pinning effect (highest magnetization).

The %MR as a function of temperature as shown in Figure 5(b) are computed from single and bi-layer thin film sample. The percentage of MR is calculated using $\%MR= (R_H-R_o/R_o) \times 100$, where R_o and R_H is the resistivity at zero and applied external magnetic field respectively. All sample exhibit negative %MR and further increase as temperature decrease. As discussed previously, the mobility of the delocalized spin (e_g) is one of the key for conduction. In an applied magnetic field, the localized and delocalized spin tends to align with the applied magnetic field direction and this enhanced the electron transfer between Mn^{3+} and Mn^{4+} via DE mechanism. At low temperature, the effect of thermal fluctuation was weakened and improves the tendency of magnetic spins to align, thus enhance the %MR. However the %MR from bi-layer films is weaker and scattered especially at low temperature compared to single layer LBMO. As discussed previously, the magnetic pinning effect occurred in LMO/LBMO and LBMO/LMO coupling. The magnetic spins are hard to align and the alignment is unstable or fluctuates when magnetic field was applied. Thus, the %MR weak and become scattered. The %MR shown by LMO/LBMO is more scattered compared to LBMO/LMO. This probably due to the higher magnetic pinning effect takes place in LMO/LBMO as compared to LBMO/LMO and caused greater fluctuation of magnetic spins when magnetic field was applied.

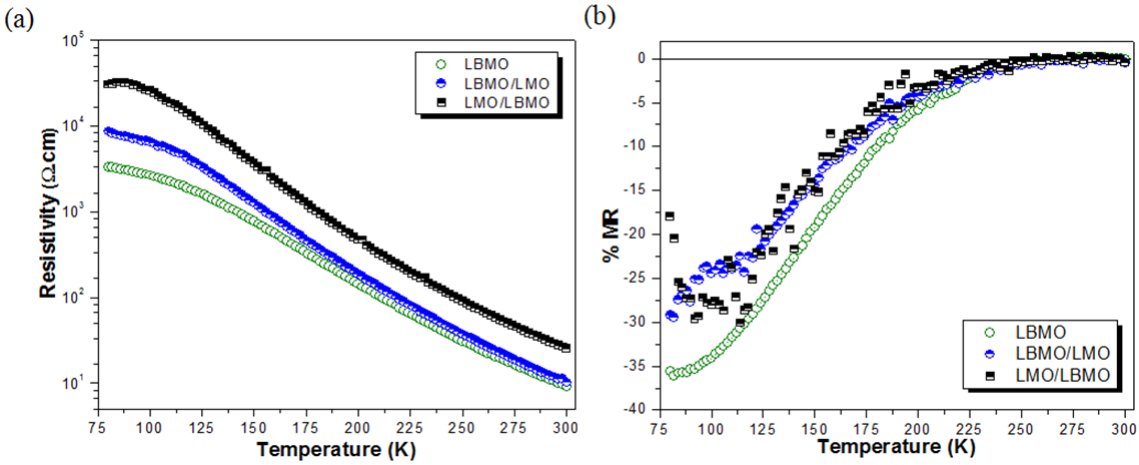

Figure 5: (a) Temperature variation of resistivity in zero magnetic field and (b) %MR as a function of temperature in 10kG of applied external magnetic field

CONCLUSION

The crystal structure formation of bi-layer thin film is strongly depends on the base to be grown due to the lattice misfit induced from bottom layer. This altered its Mn-O-Mn bond angle and length. The magnetic interactions of the bi-layer system were suppressed due to magnetic pinning effect. Such changes not only altered the electrical transport of the system but also the magnetotransport properties. The resistance is higher in bi-layer coupling while the %MR is lower and scattered at low temperature. Therefore, bi-layer manganite thin film is stacking sequence dependent.

ACKNOWLEDGMENTS

The Ministry of Higher Education Malaysia (MOHE) is gratefully acknowledged for the grant under Research University Grant Scheme (RUGS) vote 91849: Low-Field Magnetoresistance effect in polycrystalline $Ln_{1-x}A_xMnO_3$ ceramic thin films.

REFERENCES

[1]. Y. Tokura and Y. Tomioka. *Journal of Magnetism and Magnetic Materials* **200** (1999) 1-23.

[2]. S. Taran, S. Karmakar, H. Chou and B. K. Chaudhuri. *Physica Status Solidi (b)* **243** (2006) 1853-1861.

[3]. J. H. Zhang, X. G. Li and N. B. Ming. *J. Phys. D: Appl. Phys*. **35**, (2002) 1301–1304.

[4]. V. I. Mikhalov, E. E. Zubov, A. V. Pashchenko, V. N. Varyukhin , V. A. Shtaba, V. P. Dyakonov, A. Szewczyk, A. Abal'oshev, K. Piotrowski, S. J. Lewandowski, H. Szymczak and K. Dyakonov, *Low Temp. Phys.* **32**(2) (2006) 139-147.

[5]. K. A. Thomas, P. S. I. P. N. de Silva, L. F. Cohen, and A. Hossain, M. Rajeswari and T. Venkatesan, R. Hiskes, J. L. MacManus-Driscoll. *J. Appl.*

Phys. **84**(7) (1998) 3939-3948.

[6]. E. Gommert, H. Cerva, J. Wecker and K. Samwer. *J. Appl. Phys.* **85**(8) (1999) 5417-5419.

[7]. C. Kwon, K.-C. Kim, M. C. Robson, J. Y. Gu, M. Rajeswari, and T. Venkatesan. *J. Appl. Phys.* **81** (1997) 4950.

[8]. Y. P. Lee, S. Y. Park, V. G. Prokhorov, V. A. Komashko and V. L. Svetchnikov. *Applied Physics Letters* **84** (2004) 777-779.

[9]. J. Fontcuberta, B. Martinez, A. Seffar, S. Pinol, J. L. Garcia-Munoz and X. Obradors. *Physical Review Letters* **76** (1996) 1122-1125.

[10]. E.L. Nagaev. *Physics Reports* **346** (2001) 387-531.